physchem

MDPI

Article

High Pressure Raman Study of Racemic Ibuprofen Crystals

Maria-Tereza Siavou [1], Panagiotis Liakos [2], Alexandros Ioannidis [1,3], Evangelos Kyrilas [2], Niki Sorogas [1], Anna Marinopoulou [3], Andreana N. Assimopoulou [4,5], Olga Karabinaki [2], Dimitrios Christofilos [2] and John Arvanitidis [1,*]

1 Physics Department, Aristotle University of Thessaloniki, 54124 Thessaloniki, Greece; msiavou@physics.auth.gr (M.-T.S.); ioannidis8@gmail.com (A.I.); nsorogka@physics.auth.gr (N.S.)
2 School of Chemical Engineering, Laboratory of Physics, Faculty of Engineering, Aristotle University of Thessaloniki, 54124 Thessaloniki, Greece; pliakosp@cheng.auth.gr (P.L.); kyrilas.v@gmail.com (E.K.); okarabi@auth.gr (O.K.); christop@cheng.auth.gr (D.C.)
3 Department of Food Science and Technology, International Hellenic University, Alexandrian Campus, 57400 Thessaloniki, Greece; amarinop@ihu.gr
4 Laboratory of Organic Chemistry, School of Chemical Engineering, Aristotle University of Thessaloniki, 54124 Thessaloniki, Greece; adreana@cheng.auth.gr
5 Natural Products Research Center of Excellence (NatPro-AUTH), Center for Interdisciplinary Research and Innovation of Aristotle University of Thessaloniki, 57001 Thessaloniki, Greece
* Correspondence: jarvan@physics.auth.gr; Tel.: +30-2310998213

Abstract

The high pressure response and structural stability of crystalline racemic (RS) ibuprofen up to 7 GPa are explored by Raman spectroscopy, employing diamond anvil cells for the pressure application and glycerol as the pressure transmitting medium. Two independent high pressure experiments were performed with practically identical results. Both intermolecular vibrations (associated with weak van der Waals interactions and hydrogen bonding between ibuprofen molecules) and intramolecular vibrations (associated with strong covalent bonding within the ibuprofen molecule) are monitored as a function of pressure, with the former being far more susceptible to volume contraction. The pressure dependence of the Raman peak frequencies undergoes two distinct changes at ~2 and ~6 GPa, indicating the occurrence of pressure-induced structural modifications of ibuprofen. Based on the high pressure Raman data for the intermolecular vibrations of the RS ibuprofen below 2 GPa, a zero pressure value for the bulk modulus of ~7.5 GPa is also extracted.

Keywords: ibuprofen; high pressure; Raman spectroscopy; hydrogen bonds; bulk modulus

Academic Editor: Eralci Moreira Therézio

Received: 27 February 2026
Revised: 13 May 2026
Accepted: 21 May 2026
Published: 23 May 2026

1. Introduction

Ibuprofen, 2-(4-isobutylphenyl)propionic acid, is a widely used non-steroidal anti-inflammatory drug (NSAID), owing to its analgesic, anti-inflammatory, and antipyretic properties. Initially approved in the UK in 1969 as a prescription alternative to aspirin, it later became available over the counter in many countries [1,2]. Since then, it has emerged as one of the most extensively used pharmaceutical agents globally, reflecting its analgesic versatility and well-established safety profile compared with other NSAIDs [3–6]. Ibuprofen exerts its pharmacological activity through non-selective inhibition of cyclooxygenase (COX) enzymes, which are essential for prostaglandin synthesis—a key mediator of inflammation, pain, and fever [7,8]. The ibuprofen molecule ($C_{13}H_{18}O_2$) consists of an aromatic benzene ring with an isobutyl (2-methylpropyl) group attached at the para (4–) position

and a propionic acid side chain. The α-carbon of the propionic acid moiety in ibuprofen is a stereogenic center, being bonded to four different substituents, and thus gives rise to two enantiomers: R(−) ibuprofen and S(+) ibuprofen [9]. These enantiomers exhibit distinct pharmacological activities, with the S (dextrorotatory) isomer being the biologically active form, as it is primarily responsible for COX inhibition, while the R (levorotatory) isomer has little intrinsic COX activity [10,11]. The vast majority of ibuprofen is commercially available in racemic (RS) form, consisting of an equimolar mixture of the (R−) and (S+) enantiomers, owing to manufacturing simplicity and cost efficiency. However, the R isomer undergoes unidirectional metabolic inversion in vivo, resulting in partial conversion (50–60%) to the pharmacologically active S form, and thus preserving the drug's therapeutic action [12–16].

In its solid state, ibuprofen exhibits polymorphism, with the RS and S-enantiopure forms crystallizing in different monoclinic space groups and displaying distinct molecular packing and melting behavior [17,18]. In all the crystalline forms of ibuprofen, two neighbor molecules are connected through relatively strong O–H···O hydrogen bonds between carboxylic acid groups, forming cyclic hydrogen-bonded dimers that constitute the fundamental structural motif of the lattice. In the RS ibuprofen crystal, the dimerization of an R with an S molecule introduces a center of inversion symmetry, resulting to the monoclinic $P2_1/c$ space group with four molecules in the crystal unit cell ($Z = 4$) [19,20]. On the other hand, the absence of inversion symmetry in S-ibuprofen, where each molecule adopts the S configuration, leads to its crystallization in the monoclinic $P2_1$ space group ($Z = 4$) with somewhat different molecular packing and a melting temperature of 320–328 K [18,21–24]. The RS ibuprofen exists in two crystalline polymorphs belonging to the $P2_1/c$ space group: phase I and phase II [19,20,25]. Phase I, the most common phase, is thermodynamically stable up to its melting temperature of 348–358 K [18,21,22,26], whereas a metastable phase II, resulting from the recrystallization of amorphous ibuprofen (glass-transition temperature of ibuprofen: T_g~228 K) at 258–260 K or from the supercooled liquid up to 273 K, melts at 280–290 K [25–28]. In phase I, the hydrogen bond is oriented nearly perpendicular to the ibuprofen dimer chains, linking molecules from adjacent chains and thereby enhancing lattice cohesion. By contrast, in phase II, the hydrogen bond connects molecules within the same chain, resulting in reduced structural stability [24,25]. At ambient conditions, the lattice parameters of the stable phase I of the RS ibuprofen are $a = 14.674$ Å, $b = 7.895$ Å, $c = 10.735$ Å, and $\beta = 99.54°$ [29].

Molecular crystals such as ibuprofen exhibit a marked contrast between strong covalent intramolecular—within the molecule—bonds, which maintain the internal molecular structure, and much weaker intermolecular—between the molecules—interactions (e.g., van der Waals interactions and hydrogen bonding), which govern key physical properties, including structural stability and solid-state transformations [30–32]. Raman spectroscopy provides a rapid, non-destructive, and in situ probe of both the intra- and intermolecular vibrations associated with these different binding forces—the latter being located in the low frequency spectral region ($\omega < 140$ cm^{-1}) [27,31]—and is therefore widely applied in pharmaceutical research for ibuprofen identification and characterization [27,33–41]. Intermolecular interactions, owing to their relative weakness with respect to intramolecular bonding, are considerably more sensitive to external stimuli, like pressure or temperature, and this difference is directly reflected in the corresponding vibrational modes [42–45]. Lazarević et al. studied the temperature evolution of the low frequency Raman spectrum ($\omega < 200$ cm^{-1}) of the solid RS ibuprofen in the temperature range 100–300 K, combined with first principles calculations for a single ibuprofen molecule, attempting the discrimination between inter- and intramolecular vibrations within this spectral region [31]. They naturally argued that a more complete determination of vibrational mode types would require combined pressure- and temperature-dependent Raman measurements. Never-

theless, to our knowledge, there has been no systematic high pressure Raman study of ibuprofen reported in the literature to date. Instead, Ostrowska et al. examined the pressure response of the RS ibuprofen up to 4 GPa by means of single-crystal X-ray diffraction (XRD) measurements [29]. They reported that pressure primarily reduces the void volume and increases the intermolecular interactions, resulting in a more skewed configuration of the O–H···O-bonded carboxyl groups without destabilizing the crystal structure. In addition, although the monoclinic angle β monotonically increases with pressure in the regime 0–2 GPa, reaching ~100.4° at ~1.9 GPa, it remains nearly constant as the pressure further increases from 2 to 4 GPa [29].

In the present work, high pressure Raman measurements of the commercial RS ibuprofen crystals were conducted up to 7 GPa, employing diamond anvil cells for pressure application and glycerol as the pressure transmitting medium, in order to assess the response of the inter- and the intramolecular vibrational modes to volume contraction and to evaluate the structural stability of the system. Consistent with the substantial differences between the corresponding binding forces, the frequencies and relative intensities of Raman peaks attributed to intermolecular vibrations are markedly more sensitive to applied pressure than those associated with intramolecular vibrations. Moreover, distinct changes in the pressure dependence of the Raman peak frequencies—much more prominent for the Raman peaks attributed to intermolecular vibrations—are observed at ~2 and ~6 GPa, signaling the occurrence of structural changes in the ibuprofen. The former is reversible, while taking into account the aforementioned high pressure XRD data [29], it can be attributed to a structural modification of crystalline ibuprofen due to the selective enhancement of intermolecular interactions and small changes in the molecular packing upon compression. As for the latter structural change, which exhibits a small hysteretic behavior, it may also be assisted by the progressive development of non-hydrostatic conditions in the sample following solidification of the pressure transmitting medium.

2. Materials and Methods

The polycrystalline RS ibuprofen sample (phase I form—melting temperature: ~350 K) was purchased from Fagron Hellas (Trikala, Greece) and used as-received. Unpolarized Raman spectra were acquired in the backscattering geometry, employing a microscope-equipped Raman spectrometer (LabRAM HR, HORIBA, Kyoto, Japan) with a spectral width—depending on the spectral window—of 2.4–3.5 cm^{-1} (high-to-low frequency range), as determined by the selected experimental parameters (600 grooves/mm grating, 50 μm entrance pinhole, 514 nm excitation wavelength). The spectra were excited by the linearly polarized laser emission of a 514 nm diode-pumped solid-state laser (Cobolt Fandango^{TM}, HÜBNER Photonics, Kassel, Germany) at a power of ~1 mW, delivered in the high pressure chamber by a 50× (N.A. 0.45) long working distance objective (focusing spot diameter: ~2 μm) to eliminate laser-heating effects. An appropriate edge filter was used to eliminate the elastically scattered light from the sample; while, prior to each spectrum accumulation, the spectrometer was calibrated by means of a Ne reference lamp. In order to assess the sample homogeneity, several randomly oriented ibuprofen crystals with sizes of a few tens of micrometers were examined by Raman spectroscopy at ambient pressure. Apart from differentiations in their relative intensities, the majority of the Raman peaks have practically the same frequencies for the various crystals.

For the high pressure experiments, either a Mao-Bell or a gas membrane-type diamond anvil cell (DAC, Almax easyLab, Diksmuide, Belgium), equipped with ~100 μm–thick drilled (~120 μm hole diameter) stainless steel gaskets, served as the sample chambers for pressure application. The pressure was monitored by inserting ruby chips inside the sample chamber and using the well-known ruby fluorescence technique [46,47], while Raman

spectra at various pressures—upon pressure increase and decrease—were consistently collected from the same sample spot of an ibuprofen crystal. For consistency with the earlier XRD study [29], highly viscous glycerol (glycerine), which does not interact with ibuprofen crystals, was employed as the pressure transmitting medium (PTM). At room temperature, pure glycerol solidifies at ~5.5 GPa, providing good hydrostatic conditions, with the pressure standard deviation remaining below 0.015 GPa up to its solidification point. Above the solidification pressure, glycerol undergoes a glass transition and the standard deviation increases quasilinearly, reaching ~0.09 GPa at a mean pressure of ~7 GPa (the highest pressure attained in our experiments) [48,49]. Two independent high pressure experiments (Run 1 up to ~7 GPa and Run 2 up to ~5.5 GPa) on different ibuprofen crystals were performed, providing very similar results.

3. Results and Discussion

A typical Raman spectrum of the RS ibuprofen crystals examined is illustrated in Supplementary Figure S1 (Supplementary Materials), together with a schematic representation of the hydrogen-bonded ibuprofen molecular dimer and the corresponding crystal unit cell using VESTA software [29,50,51]. The complexity of the ibuprofen molecule and the relatively low symmetry of its crystalline structure in its solid state, with four molecules in the crystal unit cell, cause the appearance of a large number of densely spaced and partially overlapping Raman peaks in the experimental spectrum, extending across the entire spectral range up to ~3100 cm^{-1}. Several studies in the literature have attempted to assign experimentally observed Raman peaks to specific intramolecular vibrations using theoretical calculations focused on the individual ibuprofen molecule [31,34,52–55] and/or the hydrogen-bonded ibuprofen dimer, in which intermolecular hydrogen bonding and the associated vibrational modes also come into play [34,51,56,57]. Taking into account the existence of four ibuprofen molecules (two hydrogen-bonded dimers) in the centrosymmetric unit cell of the RS ibuprofen and correlating the translational and rotational modes of an individual molecule to the site and the crystal symmetry, 21 intermolecular (external) optical phonon modes at the Γ point of the Brillouin zone are expected with symmetry species, as follows [31,58]:

$$\Gamma_{ext} = 6A_g + 6B_g + 5A_u + 4B_u \quad (1)$$

All vibrational modes with even (gerade, g) parity under inversion are Raman active, whereas modes with odd (ungerade, u) parity are infrared (IR) active. Hence, a maximum of 12 intermolecular vibrational modes—attributed to translational and rotational motions of ibuprofen molecules as rigid bodies—is expected in the low frequency Raman spectrum of the RS ibuprofen crystals because of the weak intermolecular interactions and the heavy masses involved (molecules). Moreover, since each of the four ibuprofen molecules in the centrosymmetric unit cell consist of 33 atoms, 372 intramolecular (internal) vibrational modes are also expected with symmetries, as follows [31]:

$$\Gamma_{int} = 93A_g + 93B_g + 93A_u + 93B_u \quad (2)$$

Of these, the 93 with A_g and the 93 with B_g symmetry are also Raman active. Because of the weakness of the intermolecular interactions in the crystal, these vibrational modes typically appear in the Raman spectrum as A_g–B_g doublets with small or even negligible splitting around the corresponding frequencies of the isolated molecule vibrations [31,57]. Given the strong covalent bonding and low atomic masses involved (atoms), the intramolecular Raman-active vibrations extend over the entire spectral region up to ~3100 cm^{-1} [57].

Their exact frequencies depend on the force constants associated with each vibrational mode, which are determined by the specific bond stretching and bond bending character.

We first examined the pressure evolution of the Raman spectrum of the crystalline RS ibuprofen in the low frequency region, where the intermolecular and low frequency deformation and torsional intramolecular modes of vibration are expected [52]. In this context, the low frequency Raman spectra at representative pressures acquired from the first ibuprofen crystal (Run 1) during pressure increase are illustrated in Figure 1a, while those acquired from the second ibuprofen crystal (Run 2) are presented in Supplementary Figure S2a. It should be noted that the lowest reliably measurable frequency in these spectra (~60 cm^{-1}) is defined by the edge filter cut-off of the spectrometer employed to reject elastically scattered light from the studied sample. A comparison of the spectra recorded at relatively low pressures for the two crystals, which have different crystallographic orientations relative to the linearly polarized laser beam used for excitation, reveals Raman peaks at essentially the same frequencies but with different relative intensities. Upon pressure increase, all Raman peaks in the spectral range under consideration shift to higher frequencies with different rates, reflecting the bond stiffening (increase of the force constants) upon compression, while a redistribution of their relative intensities is also observed. The pressure-induced frequency upshifts lead to the gradual appearance of additional Raman peaks within the measured spectral window from its low frequency side. Moreover, Raman peaks that are accidentally degenerate at ambient or low pressure become resolved at higher pressures due to their different pressure-induced frequency shift rates.

At each measured pressure, the corresponding Raman spectrum was fitted with an appropriate number of Voigt functions to account for the individual Raman peak components; the pressure dependencies of all the peak frequencies are presented in Figure 1b and Supplementary Figure S2b for Run 1 and Run 2, respectively. The frequency vs. pressure data for each Raman peak was fitted in the pressure range 0–2 GPa (solid lines through the corresponding data points in the figures) using the linear or parabolic functions, as follows:

$$\omega_i = \omega_{i0} + b_1 P \text{ or } \omega_i = \omega_{i0} + b_1 P + b_2 P^2. \quad (3)$$

The corresponding linear pressure coefficients (b_1) of the frequencies of all the well-resolved Raman peaks are likewise given in Figure 1b and Supplementary Figure S2b, presented with one decimal place in the case of the linear fit and with no decimal places for the parabolic fit. These values are similar for the two individual high pressure experiments, revealing the reproducibility of our results. All the parabolic dependencies are sublinear (negative b_2 values), being indicative—in line with the previous XRD study [29]—of the initial (in the low pressure regime) rapid enhancement of the intermolecular interactions in crystalline ibuprofen. Following the Raman spectroscopic study by Lazarević et al. [31], we assign all the observed Raman peaks with zero pressure frequencies $\omega_{i0} < 130$ cm^{-1} to intermolecular phonon modes, while those with higher ω_{i0} values to intramolecular vibrations. In particular, the peaks at ω_{i0}~139 and ~145 cm^{-1} are assigned to an intramolecular A_g–B_g doublet, split by the crystal field in its solid state [31]. As expected, in the various $\omega_i(P)$ dependencies, both the b_1 values and the negative b_2 coefficients are generally larger for intermolecular vibrations than for their intramolecular counterparts, reflecting the weakness of the molecule–molecule interactions associated with the former and their strengthening upon volume contraction.

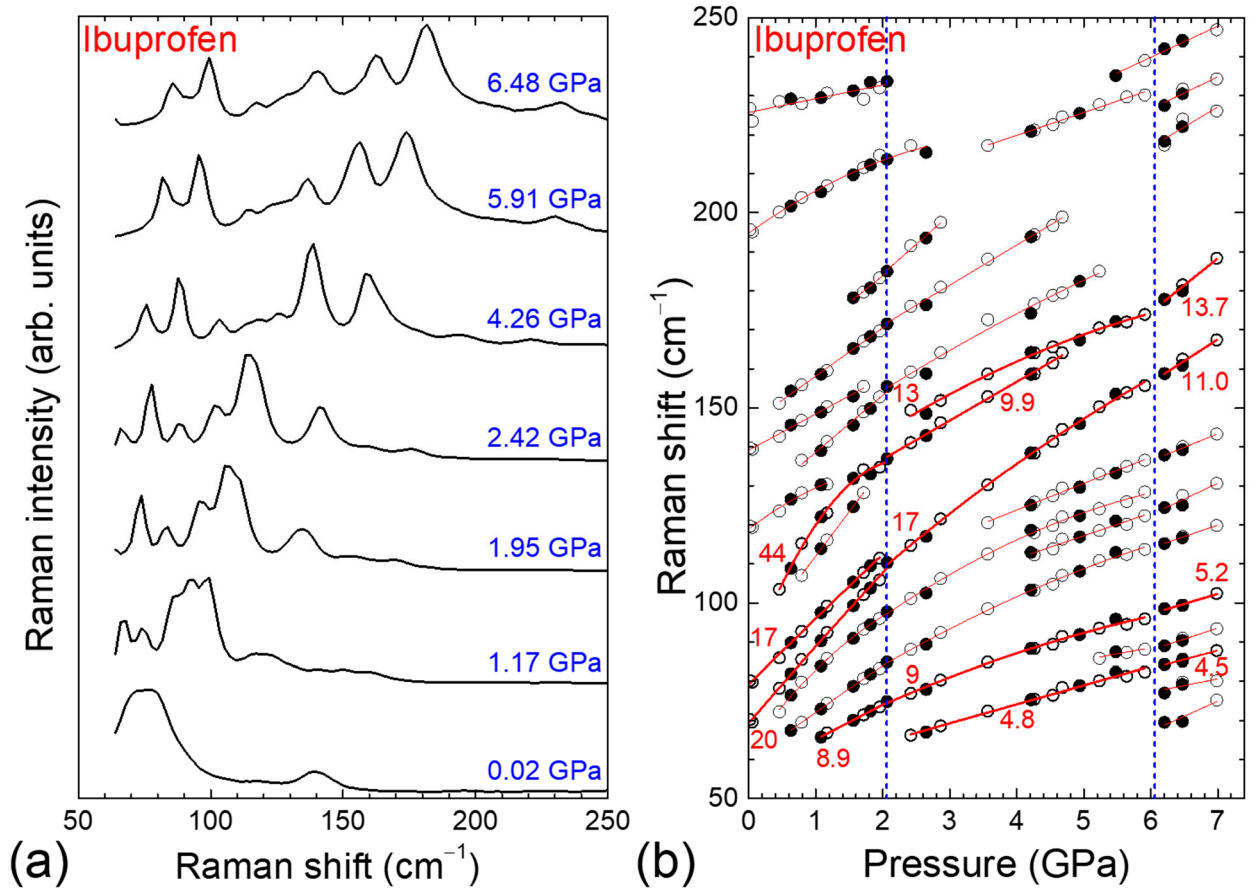

Figure 1. (**a**) Raman spectra of ibuprofen in the low frequency region ($\omega < 250$ cm^{-1}), acquired at various pressures during Run 1; (**b**) Pressure dependence of the Raman peak frequencies in this spectral region. Open (solid) symbols represent the data obtained upon compression (decompression). Solid lines represent the linear or parabolic least squares fit to the experimental data, while numbers refer to the linear pressure coefficients of the well-resolved Raman peak frequencies (highlighted by thicker symbols and lines). Vertical dashed lines denote the pressures at which changes in the pressure evolution of the Raman peak frequencies take place.

As can be inferred from Figure 1 and Supplementary Figure S2 for the two independent high pressure experiments, alterations in the pressure evolution of the Raman peak frequencies take place above approximately 2 GPa. Specifically, the frequency vs. pressure data for the majority of the Raman peaks cannot be adequately described by a single linear or parabolic function over the entire pressure range from ambient conditions to well above 2 GPa. Therefore, the ω_i–P data for each Raman peak were independently fitted in the 2–6 GPa range using the linear or parabolic functions given in Equation (3), generally yielding smaller b_1 values. The observed changes are fully reversible upon decompression (solid symbols in the figures) and indicate a progressive stiffening of the ibuprofen crystal lattice under further compression. Taking into account the aforementioned high pressure XRD study by Ostrowska et al. [29], the observed changes in the pressure dependence of the Raman peak frequencies in the low frequency spectral range can be attributed to a pressure-induced structural modification of crystalline ibuprofen. This modification involves the selective strengthening of intermolecular interactions upon compression, accompanied by subtle adjustments in molecular packing and relative molecular orientations within the lattice. In particular, according to Ostrowska et al. [29], compression predominantly reduces the intermolecular van der Waals contacts, thereby enhancing the intermolecular interactions and leading to a more skewed configuration of the O–H···O-bonded carboxyl groups, while the hydrogen atoms remain ordered within the compressed hydrogen bonds.

These structural changes modify the local interaction environment and, consequently, the effective force constants governing the vibrational modes, particularly those associated with intermolecular vibrations.

In the case of Run 1, the measurements extended up to ~7 GPa, i.e., beyond the solidification pressure of glycerol (~5.5 GPa) employed as the PTM (Figure 1). Additional alterations in the pressure coefficients of the Raman peak frequencies, primarily toward somewhat larger values, occur above ~6 GPa. These alterations are accompanied by a reduction in the intensity of the low frequency Raman spectrum of crystalline ibuprofen with respect to the higher frequency spectral regions, as well as by the appearance of new weak intramolecular peaks in the 200–250 cm^{-1} range. The emergence of additional weak Raman peaks, attributed to intramolecular vibrational modes, some possibly evolving from modes already present at lower pressures, is even more pronounced in the intermediate- and high frequency spectral ranges (vide infra). The observed changes suggest the occurrence of another pressure-induced structural modification of ibuprofen.

We next examined the pressure dependence of the intramolecular Raman peaks of the RS ibuprofen in the intermediate frequency region. Raman spectra in the 230–1725 cm^{-1} region, recorded during Run 1 upon compression, are shown at selected pressures in Figure 2a. The vast majority of the Raman peaks in this spectral range also undergo frequency upshifts under compression, although with smaller pressure rates than those of the intermolecular modes, consistent with the internal character of the corresponding vibrations. The pressure dependence of the frequencies of the more intense and well-resolved peaks in this region is presented in Figure 2b. The corresponding dependencies for all the Raman peaks, along with representative spectra at various pressures, are provided in Figure 3 and Supplementary Figures S3–S6 for Run 1, and in Supplementary Figures S7–S10 for Run 2.

From the aforementioned figures, redistribution of intensity among the various Raman peaks upon compression is evident, together with peak broadening at pressures exceeding the solidification pressure of the PTM used, possibly caused by the gradual loss of hydrostaticity within the sample chamber. The ω_i–P data for all the observed Raman peaks in the intermediate frequency region were fitted by linear functions in the pressure ranges 0–2 GPa, 2–6 GPa (Run 1 and Run 2) and 6–8 GPa (Run 1)—the corresponding data set for each peak cannot be fitted by a single linear or parabolic function in the entire pressure range—and their pressure coefficients b_1 for the well-resolved peaks are also given in the corresponding figures. The only exception from the linear ω_i–P dependence is the lowest frequency peak at 266 cm^{-1}—attributed to a torsional and C–C–C deformation intramolecular mode [52]—that exhibits a sublinear behavior (rapid hardening at lower pressures) in the pressure range 0–2 GPa.

Apparent similarities are observed in both the pressure-induced relative intensity changes up to ~5.5 GPa and the pressure coefficients derived from the two high pressure experiments (Run 1 and Run 2) performed on different RS ibuprofen crystals. Variations in the b_1 coefficients toward either lower or higher values are likewise observed for the intramolecular peaks at ~2 and ~6 GPa, in agreement with the structural modifications inferred from the low frequency, high pressure Raman data. Careful inspection of the Raman spectra shown in Supplementary Figure S6 and, in greater detail, in Figure 3 reveal that two relatively weak intramolecular peaks (marked by arrows in Figure 3a) exhibit an intriguing response to compression. In contrast to the conventional behavior observed for all other inter- and intramolecular vibrations—whose Raman frequencies progressively upshift upon volume contraction due to bond stiffening and the associated increase in force constants—these two peaks, located at ~1419 and ~1430 cm^{-1} at ambient pressure, display frequency downshifts as the pressure increases from 0 to 2 GPa. The corresponding

pressure coefficients are −0.4 and −1.4 cm^{-1} GPa^{-1}, respectively. For $P > 2$ GPa, the higher frequency peak exhibits a conventional positive frequency shift (+2.8 $cm^{-1}GPa^{-1}$ for $2 < P < 6$ GPa and +4.2 cm^{-1} GPa^{-1} for $P > 6$ GPa), whereas the lower frequency peak displays an even stronger negative shift than in the low pressure regime (−2.9 $cm^{-1}GPa^{-1}$), up to the pressure beyond which it can no longer be clearly resolved (~4.5 GPa). Although, in the case of lattice vibrational modes (intermolecular modes in molecular crystals), the existence of a negative pressure slope in their frequency shifts (mode softening) generally signals a structural instability and is often a precursor to a phase transition [59,60], the appearance of soft intramolecular modes in a molecular crystal could reflect changes in the molecular geometry, such as bond weakening and reorientation, or coupling effects between inter- and intramolecular modes (particularly when hydrogen bonding is involved) [61–63]. In the ibuprofen molecule, the Raman peaks at ~1418 and ~1430 cm^{-1} are associated with the C–C–H deformation in the propionate moiety, which is very sensitive to the formation of different molecular conformers, and the hydrogen-bonded CO–H bending vibration, respectively [52]. Hence, their peculiar behavior upon pressurization of solid ibuprofen likely reflects pressure-induced shortening and concomitant geometrical modifications of the adjacent hydrogen bonds [29]. Moreover, the stronger softening of the lower frequency peak for $P > 2$ GPa may reflect a gradual conformational change of the ibuprofen molecule upon further compression.

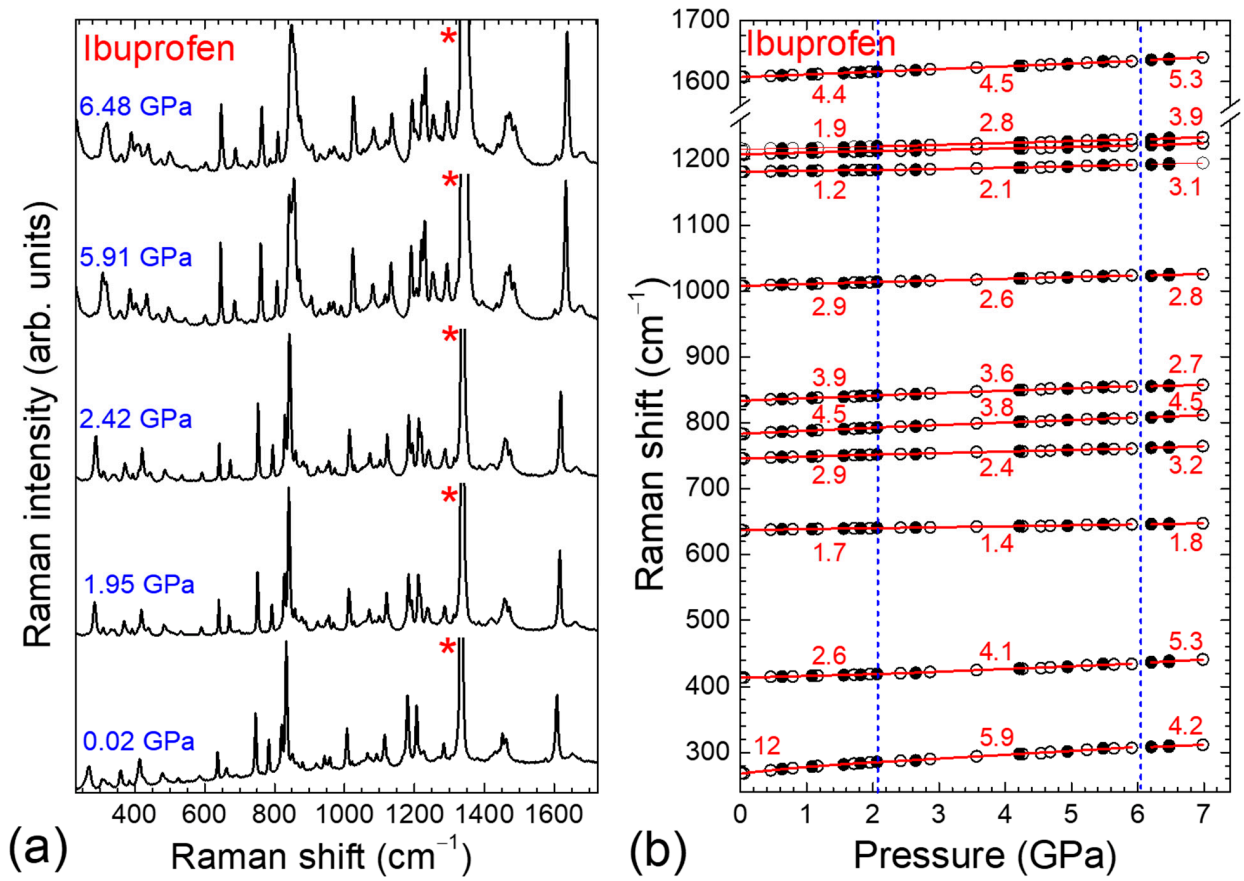

Figure 2. (**a**) Raman spectra of ibuprofen in the intermediate frequency region (230–1725 cm^{-1}), acquired at various pressures during Run 1. Asterisks mark the first order Raman peak of the diamond anvil; (**b**) Pressure dependence of the well-resolved Raman peak frequencies in this spectral region. Open (solid) symbols represent the data obtained upon compression (decompression). Solid lines represent the linear or parabolic least squares fit to the experimental data, while the numbers indicate the corresponding linear pressure coefficients. Vertical dashed lines denote the pressures at which changes in the pressure evolution of the Raman peak frequencies take place.

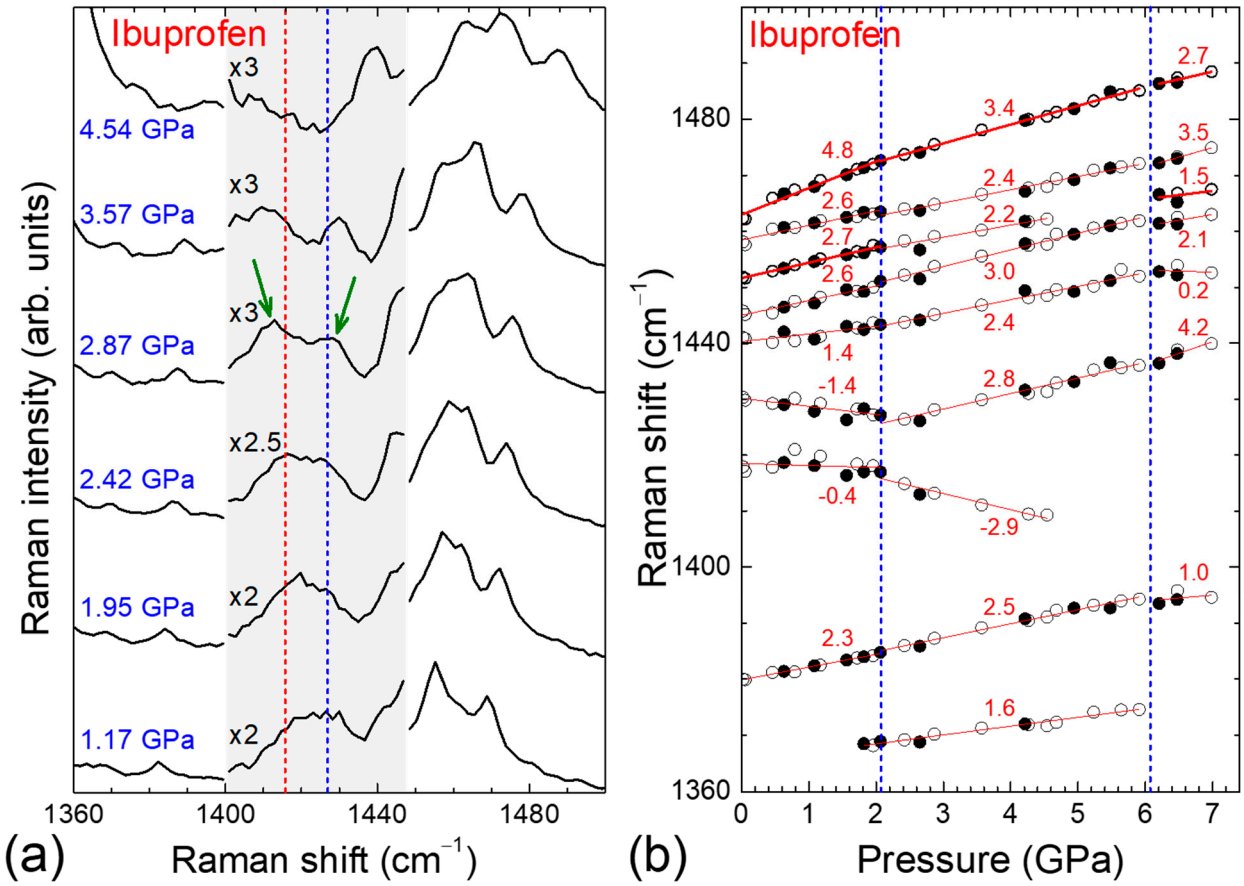

Figure 3. (**a**) Raman spectra of ibuprofen in the 1360–1500 cm^{-1} region, acquired at various pressures during Run 1. The vertical dashed lines are guides to the eye, facilitating the tracking of the pressure-induced frequency shifts of the two peaks marked by the arrows. The spectra in the spectral region around these two peaks (light grey area) were multiplied by the factors indicated in the figure to enhance visibility; (**b**) Pressure dependence of the Raman peak frequencies in this spectral region. Open (solid) symbols represent the data obtained upon compression (decompression). Solid lines represent the linear least squares fit to the experimental data, while the numbers indicate the corresponding pressure coefficients. Thick symbols and lines represent data for the well-resolved peaks. Vertical dashed lines denote the pressures at which changes in the pressure evolution of the Raman peak frequencies take place.

Regarding the higher pressure anomaly of the RS ibuprofen at ~6 GPa, reached only in Run 1, Supplementary Figures S3–S6 clearly show that, in addition to the aforementioned alterations in the pressure dependence of the Raman peak frequencies, new weak peaks emerge in the spectra. The emergence of the additional intramolecular peaks may indicate pressure-induced deformations of the molecular structure of ibuprofen. Notably, the anomalies observed at ~6 GPa—alterations in the pressure coefficients and the appearance of additional Raman peaks—exhibit, for some intramolecular modes, a small hysteretic behavior upon pressure release (solid symbols in Supplementary Figures S3–S6), as the initial lower pressure state is recovered only below 5.5 GPa. This pressure value coincides with the solidification pressure at room temperature of pure glycerol used as the PTM. Glycerol ensures good hydrostaticity for P < 5.5 GPa; however, hydrostatic conditions progressively deteriorate as the pressure increases beyond its solidification point [49]. Therefore, it can be reasonably assumed that the pressure-induced structural and molecular conformation changes of the RS ibuprofen at ~6 GPa may be assisted or even triggered by the solidification of glycerol and the consequent development of non-hydrostatic stresses on the sample.

Finally, we examined the pressure evolution of the high frequency region of the Raman spectrum of the RS ibuprofen, which encompasses the intramolecular C–H stretching vibrations as well as overtone and combination Raman modes. The corresponding data (representative Raman spectra at selected pressures and pressure dependencies of the Raman peak frequencies) are presented in Figure 4 for Run 1 and Supplementary Figure S11 for Run 2. In this spectral region, the Raman spectrum is particularly rich compared with those of many other organic materials, reflecting the non-planar nature of the ibuprofen molecule as well as the diversity of C–H bond strengths and local atomic environments. At ambient conditions, the relatively weak Raman peaks, with frequencies $\omega_{i0} < 2800$ cm^{-1} and $\omega_{i0} > 3100$ cm^{-1}, are attributed to overtones and combination modes; whereas, the stronger Raman peaks in the intermediate frequency range are assigned to C–H symmetric and antisymmetric stretching vibrations [52]. As the pressure increases, apart from a few combination Raman modes exhibiting very small or nearly zero pressure dependence, the high frequency Raman peaks upshift with relatively large pressure coefficients. The aforementioned alterations in the pressure coefficients of the first order Raman peak frequencies at ~2 GPa—primarily toward lower values—and at ~6 GPa—toward both lower and higher values—are also clearly observed and are overall more pronounced than those of the intramolecular modes in the intermediate frequency range. This behavior is consistent with the peripheral positioning of the hydrogen atoms within the ibuprofen molecular framework, which renders the C–H bonds more sensitive to pressure-induced changes in the intermolecular interactions and/or the molecular geometry.

The frequency normalized pressure slopes (logarithmic pressure coefficients) of the frequencies of the vibrational modes,

$$\Gamma_i = \partial(\ln\omega_i)/\partial P = (1/\omega_{i0})\cdot(\partial\omega_i/\partial P), \quad (4)$$

are directly proportional to the mode Grüneisen parameters, $\gamma_i = B_0\Gamma_i$, where B_0 represents the bulk modulus and ω_{i0} is the ambient pressure frequency of the *i*th mode of vibration. These quantities are useful for describing vibrational anharmonicity and for assessing the hierarchy of intermolecular and intramolecular force constants (bond strengths) in molecular crystals [42,43,45]. In molecular crystals, the Grüneisen approximation—nearly equal γ_i values for the various modes in a network crystal ($\gamma_i \approx \gamma$) and thus a uniform spectral scaling with pressure ($\omega \sim V^{-\gamma}$) [64]—is generally valid only for the intermolecular modes. However, it breaks down for intramolecular vibrations, for which an approximate $\gamma_i \sim \omega_{i0}^{-2}$ dependence is typically observed [42,43,45]. The logarithmic pressure coefficients Γ_i for $P < 2$ GPa of the Raman peak frequencies of the RS ibuprofen with respect to their frequency ω_{i0} at ambient pressure, as obtained from the Run 1 and Run 2 data, are presented in Figure 5 and Supplementary Figure S12, respectively. As can be seen from these figures, the Γ_i parameter values span almost three orders of magnitude, consistent with the coexistence of weak van der Waals intermolecular interactions and hydrogen bonding with strong covalent intramolecular bonds.

The Γ_i parameters have an average value of 0.261 GPa^{-1} for the RS ibuprofen crystal examined during Run 1 (0.269 GPa^{-1} for Run 2) for the intermolecular modes (solid blue lines in Figure 5 and Supplementary Figure S12), while for the intramolecular modes with $\omega_{i0} < 900$ cm^{-1}, they indeed approximately follow a $\gamma_i \sim \omega_{i0}^{-2}$ dependence (solid olive lines in Figure 5 and Supplementary Figure S12). For the higher frequency intramolecular modes, the Γ_i parameter values are again nearly constant (~0.003 GPa^{-1}, dashed blue lines in Figure 5 and Supplementary Figure S12), suggesting comparable force constants for these vibrations. Since compression is mainly accommodated by the reduction of intermolecular voids [29], the ambient pressure bulk modulus can be estimated from the average intermolecular Γ_i value (Γ) by means of the $\gamma = B_0\Gamma$ expression. Assuming

a reasonable value of γ~2 [42,43,45], an average value of B_0~7.5 GPa (B_0~7.7 GPa for Run 1 and B_0~7.4 GPa for Run 2) is extracted. This result shows excellent agreement with theoretical calculations, which predicted a bulk modulus of 7.74 GPa for crystalline ibuprofen [65].

The bulk modulus value for the RS ibuprofen crystals is somewhat larger than that estimated using the same experimental method for crystalline fluorene and fluoranthene with purely van der Waals intermolecular interactions between quasiplanar molecules (~7 GPa [44,66], consistent with the corresponding volume contraction data with pressure and the high pressure XRD data [67,68]). However, it is smaller than those for the van der Waals crystals of the spiro compound 9,9′-spirobifluorene (~9 GPa [69]) with smaller intermolecular voids (larger bulk modulus) as well as the hydrogen-bonded α-*trans*-cinnamic acid crystals (~11 GPa [45]). In the latter case, the structural units also consist of hydrogen-bonded molecular dimers formed between carboxyl groups across centers of symmetry, but in nearly planar configuration [70,71]. Consequently, the nearly perpendicular orientation of the hydrogen bonds relative to the dimer chains in the RS ibuprofen, combined with the pressure-induced increase in the skewness of the carboxylic linkage within the molecular dimers, may contribute to the lower stiffness of the studied material.

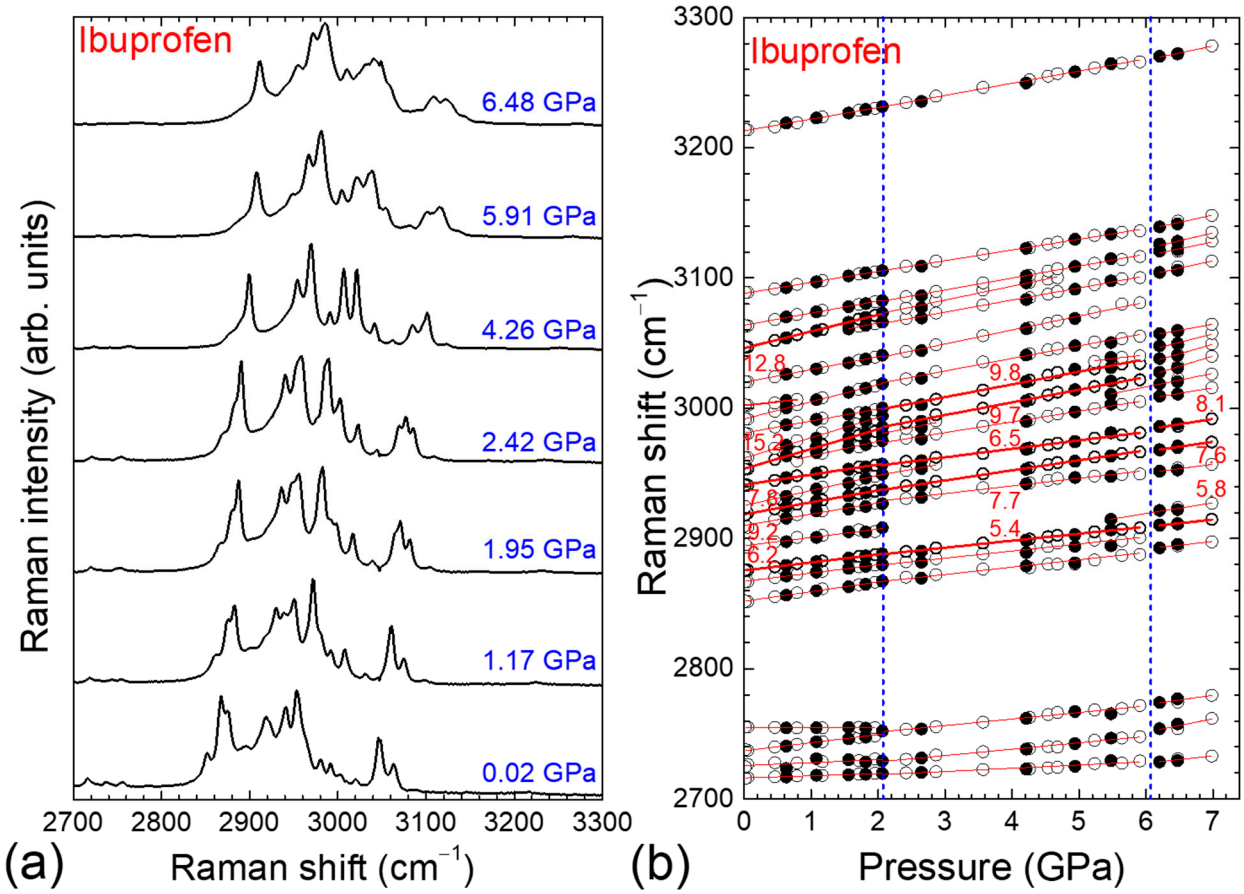

Figure 4. (**a**) Raman spectra of ibuprofen in the high frequency region (2700–3300 cm^{-1}), acquired at various pressures during Run 1; (**b**) Pressure dependence of the Raman peak frequencies in this spectral region. Open (solid) symbols represent the data obtained upon compression (decompression). Solid lines represent the linear least squares fit to the experimental data, while numbers refer to the pressure coefficients of the well-resolved Raman peak frequencies (highlighted by thicker symbols and lines). Vertical dashed lines denote the pressures at which changes in the pressure evolution of the Raman peak frequencies take place.

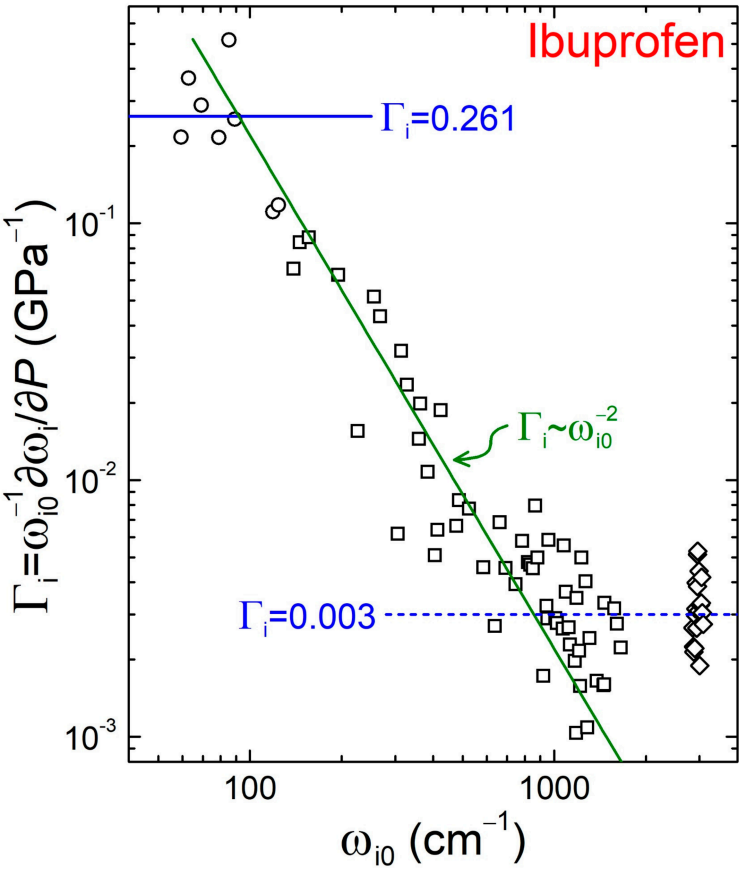

Figure 5. Logarithmic pressure coefficients Γ_i of the Raman peak frequencies of ibuprofen, obtained from Run 1 for $P < 2$ GPa, plotted as a function of their ambient pressure frequencies ω_{i0}. Circles, squares, and rhombi correspond to the intermolecular, intermediate frequency intramolecular, and C–H stretching modes of vibration, respectively. The horizontal blue lines correspond to the averaged values $\Gamma_i = 0.261$ GPa^{-1} for the intermolecular (solid line) and $\Gamma_i = 0.003$ GPa^{-1} for the high frequency ($\omega_{i0} > 900$ cm^{-1}) intramolecular vibrations (dashed line). The solid green line through the data for the intermediate frequency intramolecular vibrations corresponds to the $\Gamma_i \sim \omega_{i0}^{-2}$ dependence.

4. Conclusions

In summary, we reported a detailed high pressure Raman investigation of racemic ibuprofen (phase I) crystals up to 7 GPa, employing glycerol as the pressure transmitting medium. The intermolecular vibrational modes—governed by weak van der Waals interactions and hydrogen bonding—are significantly more sensitive to compression than the intramolecular modes associated with strong covalent bonding. Two distinct modifications in the pressure dependence of the Raman peak frequencies are identified at ~2 and ~6 GPa. The former is attributed to subtle adjustments in molecular packing and relative molecular orientations, whereas the latter likely involves molecular conformational changes, possibly influenced by the onset of non-hydrostatic stresses following glycerol solidification at ~5.5 GPa. From the ω_i–P data below 2 GPa for the low frequency-lying intermolecular modes, an average bulk modulus of ~7.5 GPa is obtained for solid ibuprofen at ambient conditions, underscoring the critical role of the hydrogen bond network topology in determining the mechanical stiffness of molecular crystals.

Supplementary Materials: The following supporting information can be downloaded at: https://www.mdpi.com/article/10.3390/physchem6020030/s1. Figure S1: Typical ambient pressure Raman spectrum of racemic ibuprofen crystals, excited at 514 nm. Insets show schematic representations of the hydrogen-bonded molecular dimer of ibuprofen and the corresponding crystal unit cell using

VESTA software [29,50,51]. Figure S2: (a) Raman spectra of ibuprofen in the low frequency region (ω < 250 cm^{-1}), acquired at various pressures during Run 2. The spectrum at P = 2.62 GPa was acquired upon pressure release (downstroke); (b) Pressure dependence of the Raman peak frequencies in this spectral region. Open (solid) symbols represent the data obtained upon compression (decompression). Solid lines represent the linear or parabolic least squares fit to the experimental data, while numbers refer to the linear pressure coefficients of the well-resolved Raman peak frequencies (highlighted by thicker symbols and lines). Vertical dashed line denotes the pressure at which changes in the pressure evolution of the Raman peak frequencies take place. Figure S3: (a) Raman spectra of ibuprofen in the 240–560 cm^{-1} region, acquired at various pressures during Run 1; (b) Pressure dependence of the Raman peak frequencies in this spectral region. Open (solid) symbols represent the data obtained upon compression (decompression). Solid lines represent the linear or parabolic least squares fit to the experimental data, while numbers refer to the linear pressure coefficients of the well-resolved Raman peak frequencies (highlighted by thicker symbols and lines). Vertical dashed lines denote the pressures at which changes in the pressure evolution of the Raman peak frequencies take place. Figure S4: (a) Raman spectra of ibuprofen in the 560–940 cm^{-1} region, acquired at various pressures during Run 1; (b) Pressure dependence of the Raman peak frequencies in this spectral region. Open (solid) symbols represent the data obtained upon compression (decompression). Solid lines represent the linear least squares fit to the experimental data, while numbers refer to the pressure coefficients of the well-resolved Raman peak frequencies (highlighted by thicker symbols and lines). Vertical dashed lines denote the pressures at which changes in the pressure evolution of the Raman peak frequencies take place. Figure S5: (a) Raman spectra of ibuprofen in the 900–1320 cm^{-1} region, acquired at various pressures during Run 1; (b) Pressure dependence of the Raman peak frequencies in this spectral region. Open (solid) symbols represent the data obtained upon compression (decompression). Solid lines represent the linear least squares fit to the experimental data, while numbers refer to the pressure coefficients of the well-resolved Raman peak frequencies (highlighted by thicker symbols and lines). Vertical dashed lines denote the pressures at which changes in the pressure evolution of the Raman peak frequencies take place. Figure S6: (a) Raman spectra of ibuprofen in the 1300–1700 cm^{-1} region, acquired at various pressures during Run 1. Asterisks mark the first order Raman peak of the diamond anvil; (b) Pressure dependence of the Raman peak frequencies in this spectral region. Open (solid) symbols represent the data obtained upon compression (decompression). Solid lines represent the linear least squares fit to the experimental data, while numbers refer to the pressure coefficients of the well-resolved Raman peak frequencies (highlighted by thicker symbols and lines). Vertical dashed lines denote the pressures at which changes in the pressure evolution of the Raman peak frequencies take place. Figure S7: (a) Raman spectra of ibuprofen in the 240–560 cm^{-1} region, acquired at various pressures during Run 2. The spectrum at P = 2.62 GPa was acquired upon pressure release (downstroke); (b) Pressure dependence of the Raman peak frequencies in this spectral region. Open (solid) symbols represent the data obtained upon compression (decompression). Solid lines represent the linear or parabolic least squares fit to the experimental data, while numbers refer to the linear pressure coefficients of the well-resolved Raman peak frequencies (highlighted by thicker symbols and lines). Vertical dashed line denotes the pressure at which changes in the pressure evolution of the Raman peak frequencies take place. Figure S8: (a) Raman spectra of ibuprofen in the 560–940 cm^{-1} region, acquired at various pressures during Run 2. The spectrum at P = 2.62 GPa was acquired upon pressure release (downstroke); (b) Pressure dependence of the Raman peak frequencies in this spectral region. Open (solid) symbols represent the data obtained upon compression (decompression). Solid lines represent the linear least squares fit to the experimental data, while numbers refer to the pressure coefficients of the well-resolved Raman peak frequencies (highlighted by thicker symbols and lines). Vertical dashed line denotes the pressure at which changes in the pressure evolution of the Raman peak frequencies take place. Figure S9: (a) Raman spectra of ibuprofen in the 900–1320 cm^{-1} region, acquired at various pressures during Run 2. The spectrum at P = 2.62 GPa was acquired upon pressure release (downstroke); (b) Pressure dependence of the Raman peak frequencies in this spectral region. Open (solid) symbols represent the data obtained upon compression (decompression). Solid lines represent the linear least squares fit

to the experimental data, while numbers refer to the pressure coefficients of the well-resolved Raman peak frequencies (highlighted by thicker symbols and lines). Vertical dashed line denotes the pressure at which changes in the pressure evolution of the Raman peak frequencies take place. Figure S10: (a) Raman spectra of ibuprofen in the 1300–1700 cm^{-1} region, acquired at various pressures during Run 2. The spectrum at P = 2.62 GPa was acquired upon pressure release (downstroke). Asterisks mark the first order Raman peak of the diamond anvil; (b) Pressure dependence of the Raman peak frequencies in this spectral region. Open (solid) symbols represent the data obtained upon compression (decompression). Solid lines represent the linear least squares fit to the experimental data, while numbers refer to the pressure coefficients of the well-resolved Raman peak frequencies (highlighted by thicker symbols and lines). Vertical dashed line denotes the pressure at which changes in the pressure evolution of the Raman peak frequencies take place. Figure S11: (a) Raman spectra of ibuprofen in the high frequency region (2700–3300 cm^{-1}), acquired at various pressures during Run 2. The spectrum at P = 2.62 GPa was acquired upon pressure release (downstroke); (b) Pressure dependence of the Raman peak frequencies in this spectral region. Open (solid) symbols represent the data obtained upon compression (decompression). Solid lines represent the linear least squares fit to the experimental data, while numbers refer to the linear pressure coefficients of the well-resolved Raman peak frequencies (highlighted by thicker symbols and lines). Vertical dashed line denotes the pressure at which changes in the pressure evolution of the Raman peak frequencies take place. Figure S12: Logarithmic pressure coefficients Γ_i of the Raman peak frequencies of ibuprofen, obtained from Run 2 for P < 2 GPa, plotted as a function of their ambient pressure frequencies ω_{i0}. Circles, squares, and rhombi correspond to the intermolecular, intermediate frequency intramolecular and C–H stretching modes of vibration, respectively. The horizontal blue lines correspond to the averaged values Γ_i = 0.269 GPa^{-1} for the intermolecular (solid line) and Γ_i = 0.003 GPa^{-1} for the high frequency (ω_{i0} > 900 cm^{-1}) intramolecular vibrations (dashed line). The solid green line through the data for the intermediate frequency intramolecular vibrations corresponds to the $\Gamma_i \sim \omega_{i0}^{-2}$ dependence.

Author Contributions: Conceptualization, M.-T.S., A.M. and J.A.; methodology, D.C. and J.A.; formal analysis, M.-T.S., P.L., A.I., O.K. and J.A.; investigation, M.-T.S., P.L., A.I., E.K., N.S., O.K., D.C. and J.A.; resources, A.M., A.N.A., D.C. and J.A.; writing—original draft preparation, M.-T.S. and J.A.; writing—review and editing, A.M., A.N.A., O.K., D.C. and J.A.; visualization, O.K. and J.A.; supervision, J.A.; project administration, D.C. and J.A. All authors have read and agreed to the published version of the manuscript.

Funding: This research received no external funding.

Data Availability Statement: The original contributions presented in this study are included in the article/Supplementary Material. Further inquiries can be directed to the corresponding author.

Acknowledgments: The authors acknowledge the Center of Interdisciplinary Research and Innovation of the Aristotle University of Thessaloniki (CIRI–AUTH) for the access to the Raman instrumentation.

Conflicts of Interest: The authors declare no conflicts of interest.

Abbreviations

The following abbreviations are used in this manuscript:

NSAID	Nonsteroidal anti-inflammatory drug
COX	Cyclooxygenase
RS	Racemic
PTM	Pressure transmitting medium
XRD	X-ray diffraction
DAC	Diamond anvil cell
IR	Infrared

References

1. Moore, N. Ibuprofen: A journey from prescription to over-the-counter use. *J. R. Soc. Med.* **2007**, *100*, 2–6. [CrossRef] [PubMed]
2. Halford, G.M.; Lordkipanidzé, M.; Watson, S.P. 50th anniversary of the discovery of ibuprofen: An interview with Dr Stewart Adams. *Platelets* **2012**, *23*, 415–422. [CrossRef]
3. Busson, M. Update on ibuprofen: Review article. *J. Int. Med. Res.* **1986**, *14*, 53–62. [CrossRef]
4. Rainsford, K.D. Ibuprofen: Pharmacology, efficacy and safety. *Inflammopharmacology* **2009**, *17*, 275–342. [CrossRef]
5. Varrassi, G.; Pergolizzi, J.V.; Dowling, P.; Paladini, A. Ibuprofen safety at the golden anniversary: Are all NSAIDs the same? A narrative review. *Adv. Ther.* **2020**, *37*, 61–82. [CrossRef]
6. Shinde, J.B.; Ingole, R.D.; Shaikh, U.A.; Khan, M.K.; Giram, S.D.; Gaikwad, S.B.; Ingole, A.P. Review on: Comparative efficacy of ibuprofen over other NSAIDs. *Int. J. Pharm. Sci.* **2025**, *3*, 3571–3579. [CrossRef]
7. Bushra, R.; Aslam, N. An overview of clinical pharmacology of ibuprofen. *Oman Med. J.* **2010**, *25*, 155–161. [CrossRef]
8. Ainyanbhor, I.E.; Edo, G.I.; Ali, A.B.M.; Akpoghelie, P.O.; Akpo, M.O.; Yousif, E.; Owheruo, J.O.; Igbuku, U.A.; Obayomi, O.V.; Essaghah, A.E.A.; et al. Ibuprofen: A review on its synthesis, mechanism of action, pharmacological properties, and environmental impact. *Pharmacol. Res.-Rep.* **2025**, *4*, 100066. [CrossRef]
9. Huang, X.; Orimoto, Y.; Aoki, Y. Theoretical examination on the chiral separation mechanism of ibuprofen on cellulose tris(4-methylbenzoate). *Molecules* **2025**, *30*, 3503. [CrossRef]
10. Boneberg, E.M.; Zou, M.H.; Ullrich, V. Inhibition of cyclooxygenase-1 and -2 by R(−)– and S(+)–ibuprofen. *J. Clin. Pharmacol.* **1996**, *36*, 16S–19S. [CrossRef] [PubMed]
11. Gliszczyńska, A.; Sánchez-López, E. Dexibuprofen therapeutic advances: Prodrugs and nanotechnological formulations. *Pharmaceutics* **2021**, *13*, 414. [CrossRef]
12. Adams, S.S.; Bresloff, P.; Mason, C.G. Pharmacological differences between the optical isomers of ibuprofen: Evidence for metabolic inversion of the (–)–isomer. *J. Pharm. Pharmacol.* **1976**, *28*, 256–257. [CrossRef]
13. Evans, A.M. Comparative pharmacology of S(+)–ibuprofen and (RS)–ibuprofen. *Clin. Rheumatol.* **2001**, *20*, S9–S14. [CrossRef] [PubMed]
14. Hao, H.; Wang, G.; Sun, J. Enantioselective pharmacokinetics of ibuprofen and involved mechanisms. *Drug Metab. Rev.* **2005**, *37*, 215–234. [CrossRef] [PubMed]
15. Ikuta, H.; Kawase, A.; Iwaki, M. Stereoselective pharmacokinetics and chiral inversion of ibuprofen in adjuvant-induced arthritic rats. *Drug Metab. Dispos.* **2017**, *45*, 316–324. [CrossRef]
16. Yang, H.; Li, Y.; Xu, C.; Li, J. The stereoselective pharmacokinetics of ibuprofen enantiomers in mice, guinea pigs, and rats. *Chirality* **2026**, *38*, e70081. [CrossRef]
17. Leising, G.; Resel, R.; Stelzer, F.; Tasch, S.; Lanziner, A.; Hantich, G. Physical aspects of dexibuprofen and racemic ibuprofen. *J. Clin. Pharmacol.* **1996**, *36*, 3S–6S. [CrossRef]
18. Lerdkanchanaporn, S.; Dollimore, D. A thermal analysis study of ibuprofen. *J. Therm. Anal. Calorim.* **1997**, *49*, 879–886. [CrossRef]
19. Shankland, N.; Wilson, C.C.; Florence, A.J.; Cox, P.J. Refinement of ibuprofen at 100K by single-crystal pulsed neutron diffraction. *Acta Cryst. C* **1997**, *53*, 951–954. [CrossRef]
20. King, M.D.; Buchanan, W.D.; Korter, T.M. Understanding the terahertz spectra of crystalline pharmaceuticals: Terahertz spectroscopy and solid-state density functional theory study of (S)–(+)–ibuprofen and (RS)–ibuprofen. *J. Pharm. Sci.* **2011**, *100*, 1116–1129. [CrossRef] [PubMed]
21. Romero, A.J.; Rhodes, T. Approaches to stereospecific preformulation of ibuprofen. *Drug Dev. Ind. Pharm.* **1991**, *17*, 777–792. [CrossRef]
22. Romero, A.J.; Rhodes, T. Stereochemical aspects of the molecular pharmaceutics of ibuprofen. *J. Pharm. Pharmacol.* **1993**, *45*, 258–262. [CrossRef]
23. Freer, A.A.; Bunyan, J.M.; Shankland, N.; Sheen, D.B. Structure of (S)–(+)–ibuprofen. *Acta Cryst. C* **1993**, *49*, 1378–1380. [CrossRef]
24. Bernal, I.; Lalancette, R. Ibuprofen, a household pharmaceutical belonging to the racemic mimic class-chirality, diastereochemical details, packing and overlay of the pair within the (S)(+) crystals. *Eur. J. Chem.* **2025**, *16*, 327–330. [CrossRef]
25. Derollez, P.; Dudognon, E.; Affouard, F.; Danède, F.; Correia, N.T.; Descamps, M. Ab initio structure determination of phase II of racemic ibuprofen by X-ray powder diffraction. *Acta Cryst. B* **2010**, *66*, 76–80. [CrossRef] [PubMed]
26. Dudognon, E.; Danède, F.; Descamps, M.; Correia, N.T. Evidence for a new crystalline phase of racemic ibuprofen. *Pharm. Res.* **2008**, *25*, 2853–2858. [CrossRef]
27. Hédoux, A.; Guinet, Y.; Derollez, P.; Dudognon, E.; Correia, N.T. Raman spectroscopy of racemic ibuprofen: Evidence of molecular disorder in phase II. *Int. J. Pharm.* **2011**, *421*, 45–52. [CrossRef]
28. Williams, P.A.; Hughes, C.E.; Harris, K.D.M. New insights into the preparation of the low-melting polymorph of racemic ibuprofen. *Cryst. Growth Des.* **2012**, *12*, 5839–5845. [CrossRef]
29. Ostrowska, K.; Kropidłowska, M.; Katrusiak, A. High-pressure crystallization and structural transformations in compressed R,S-ibuprofen. *Cryst. Growth Des.* **2015**, *15*, 1512–1517. [CrossRef]

30. Desiraju, G.R. *Crystal Engineering: The Design of Organic Solids*; Elsevier Scientific Publishers: New York, NY, USA, 1989.
31. Lazarević, J.J.; Uskoković-Marković, S.; Jelikić-Stankov, M.; Radonjić, M.; Tanasković, D.; Lazarević, N.; Popović, Z.V. Intermolecular and low-frequency intramolecular Raman scattering study of racemic ibuprofen. *Spectrochim. Acta A* **2014**, *126*, 301–305. [CrossRef]
32. Yin, X.; Liu, J.; Wei, Y.; Meng, X.; Zhang, H. Terahertz spectral of RS-ibuprofen and its enantiomer S–(+)–ibuprofen. *J. Photochem. Photobiol. A* **2026**, *473*, 116866. [CrossRef]
33. Breitenbach, J.; Schrof, W.; Neumann, J. Confocal Raman-spectroscopy: Analytical approach to solid dispersions and mapping of drugs. *J. Pharm. Res.* **1999**, *16*, 1109–1113. [CrossRef]
34. Rossi, B.; Verrocchio, P.; Viliani, G.; Mancini, I.; Guella, G.; Rigo, E.; Scarduellia, G.; Mariotto, G. Vibrational properties of ibuprofen-cyclodextrin inclusion complexes investigated by Raman scattering and numerical simulation. *J. Raman Spectrosc.* **2009**, *40*, 453–458. [CrossRef]
35. Fini, A.; Cavallari, C.; Ospitali, F. Effect of ultrasound on the compaction of ibuprofen/isomalt systems. *Pharmaceutics* **2009**, *1*, 3–19. [CrossRef]
36. Omar, J.; Ana Boix, A.; Ulberth, F. Raman spectroscopy for quality control and detection of substandard painkillers. *Vib. Spectrosc.* **2020**, *111*, 103147. [CrossRef]
37. Gómez, S.; Rojas-Valencia, N.; Giovannini, T.; Restrepo, A.; Cappelli, C. Ring vibrations to sense anionic ibuprofen in aqueous solution as revealed by resonance Raman. *Molecules* **2022**, *27*, 442. [CrossRef] [PubMed]
38. Guinet, Y.; Paccou, L.; Hédoux, A. Low-frequency Raman spectroscopy: An exceptional tool for exploring metastability driven states induced by dehydration. *Pharmaceutics* **2023**, *15*, 1955. [CrossRef]
39. Gómez-Castillo, N.Y.; Sallo-Chabla, N.J.; Pérez-Zárate, D.; Bósquez-Cáceres, M.F.; Chacón-Torres, J.C. Graphene-enhanced Raman spectroscopy in ultra-low concentrations of pharmaceuticals. *Carbon Trends* **2025**, *20*, 100505. [CrossRef]
40. Bui Bao Duy, B.B.; Khanh, H.M.; Tram, L.T.B.; Minh, D.T.C. Determination of ibuprofen content in tablets using Raman spectroscopy. *Hue J. Med. Pharm.* **2025**, *15*, 19–26. [CrossRef]
41. Bhimrao, L.S.; Kumar, S.; Agrawal, A.K.; De Beer, T.; Kumar, A.; Kumar, D. Continuous manufacturing in pharmaceuticals: An integrated approach with NIR and Raman as PAT tools. *Int. J. Pharm.* **2026**, *689*, 126478. [CrossRef]
42. Zallen, R. Pressure-Raman effects and vibrational scaling laws in molecular crystals: S_8 and As_2S_3. *Phys. Rev. B* **1974**, *9*, 4485–4496. [CrossRef]
43. Zallen, R.; Slade, M.L. Influence of pressure and temperature on phonons in molecular chalcogenides: Crystalline As_4S_4 and S_4N_4. *Phys. Rev. B* **1978**, *18*, 5775–5798. [CrossRef]
44. Terzidou, A.G.V.; Sorogas, N.; Pinakidou, F.; Paloura, E.C.; Arvanitidis, J. The pressure-induced structural phase transition of fluorene studied by Raman spectroscopy. *Vib. Spectrosc.* **2021**, *115*, 103272. [CrossRef]
45. Marinopoulou, A.; Christopoulou, V.; Karabinaki, O.; Christofilos, D.; Arvanitidis, J. The high-pressure response of *trans*-cinnamic acid crystals studied by Raman spectroscopy. *Appl. Res.* **2024**, *3*, e202300129. [CrossRef]
46. Piermarini, G.J.; Block, S.; Barnett, J.D.; Forman, R.A. Calibration of the pressure dependence of the R_1 ruby fluorescence line to 195 kbar. *J. Appl. Phys.* **1975**, *46*, 2774–2780. [CrossRef]
47. Mao, H.K.; Xu, J.; Bell, P.M. Calibration of the ruby pressure gauge to 800 kbar under quasi-hydrostatic conditions. *J. Geophys. Res.* **1986**, *91*, 4673–4676. [CrossRef]
48. Osakabe, T.; Kakurai, K. Feasibility tests on pressure-transmitting media for single-crystal magnetic neutron diffraction under high pressure. *Jpn. J. Appl. Phys.* **2008**, *47*, 6544–6547. [CrossRef]
49. Klotz, S.; Takemura, K.; Strassle, T.; Hansen, T. Freezing of glycerol-water mixtures under pressure. *J. Phys. Condens. Matter* **2012**, *24*, 325103. [CrossRef]
50. Momma, K.; Izumi, F. VESTA 3 for three-dimensional visualization of crystal, volumetric and morphology data. *J. Appl. Crystallogr.* **2011**, *44*, 1272–1276. [CrossRef]
51. Demkin, A.G.; Kolesov, B.A. Tautomeric hydrogen bond in dimers of ibuprofen. *J. Phys. Chem. A* **2019**, *123*, 5537–5541. [CrossRef]
52. Vueba, M.L.; Pina, M.E.; Batista de Carvalho, L.A.E. Conformational stability of ibuprofen: Assessed by DFT calculations and optical vibrational spectroscopy. *J. Pharm. Sci.* **2008**, *97*, 845–859. [CrossRef]
53. Jubert, A.; Legarto, M.L.; Massa, N.E.; Tévez, L.L.; Okulik, N.B. Vibrational and theoretical studies of non-steroidal anti-inflammatory drugs Ibuprofen [2-(4-isobutylphenyl)propionic acid]; Naproxen [6-methoxy-α-methyl-2-naphthalene acetic acid] and Tolmetin acids [1-methyl-5-(4-methylbenzoyl)-1H-pyrrole-2-acetic acid]. *J. Mol. Struct.* **2006**, *783*, 34–51. [CrossRef]
54. Bondesson, L.; Mikkelsen, K.V.; Luo, Y.; Garberg, P.; Ågren, H. Hydrogen bonding effects on infrared and Raman spectra of drug molecules. *Spectrochim. Acta A* **2007**, *66*, 213–224. [CrossRef] [PubMed]
55. Logacheva, K.; Gergelezhiu, P.; Raksha, E.; Savostina, L.; Arzumanyan, G.; Eresko, A.; Malakhov, S.; Mamatkulov, K.; Ponomareva, O.; Belushkin, A.; et al. Vibrational spectroscopic features of ibuprofen and ketoprofen: IR and Raman spectroscopy combined with DFT calculations. *Phys. Part. Nucl. Lett.* **2024**, *21*, 839–842. [CrossRef]

56. Crupi, V.; Fontana, A.; Giarola, M.; Guella, G.; Majolino, D.; Mancini, I.; Mariotto, G.; Paciaroni, A.; Rossi, B.; Venuti, V. Cyclodextrin-complexation effects on the low-frequency vibrational dynamics of ibuprofen by combined inelastic light and neutron scattering experiments. *J. Phys. Chem. B* **2013**, *117*, 3917–3926. [CrossRef]
57. Gergelezhiu, P.; Raksha, E.; Savostina, L.; Arzumanyan, G.; Eresko, A.; Malakhov, S.; Mamatkulov, K.; Ponomareva, O.; Belushkin, A.; Chudoba, D. Structure and dynamics investigation of ibuprofen dimers by DFT method. *Phys. Part. Nucl. Lett.* **2025**, *22*, 1102–1105. [CrossRef]
58. Fateley, W.G. *Infrared and Raman Selection Rules for Molecular and Lattice Vibrations: The Correlation Method*; Wiley Interscience: New York, NY, USA, 1972.
59. Edwards, C.M.; Butler, I.S. Pressure-tuning spectroscopy of inorganic compounds: A summary of the past 15 years. *Coord. Chem. Rev.* **2000**, *199*, 1–53. [CrossRef]
60. Errandonea, D.; Martínez-García, D.; Segura, A.; Haines, J.; Machado-Charry, E.; Canadell, E.; Chervin, J.C.; Chevy, A. High-pressure electronic structure and phase transitions in monoclinic InSe: X-ray diffraction, Raman spectroscopy, and density functional theory. *Phys. Rev. B* **2008**, *77*, 045208. [CrossRef]
61. Meletov, K.P.; Maksimov, A.A.; Tartakovskii, I.I. Energy spectrum and phase transitions in C_{70} fullerite crystals at high pressure. *J. Exp. Theor. Phys.* **1997**, *84*, 144–150. [CrossRef]
62. Loi, M.A.; Cai, Q.; Chandrasekhar, H.R.; Chandrasekhar, M.; Graupner, W.; Bongiovanni, G.; Mura, A.; Botta, C.; Garnier, F. High pressure study of the intramolecular vibrational modes in sexithiophene single crystals. *Synth. Met.* **2001**, *116*, 321–326. [CrossRef]
63. Liang, A.; Turnbull, R.; Errandonea, D. A review on the advancements in the characterization of the high-pressure properties of iodates. *Prog. Mater. Sci.* **2023**, *136*, 101092. [CrossRef]
64. Jalal, S.K. Pressure dependence of lattice vibrations and phonons. In *High-Pressure Thermoelastic and Thermophysical Properties of Smart Materials*; Pandey, A.K., Dixit, C.K., Srivastava, S., Eds.; Elsevier: Amsterdam, The Netherlands, 2025; pp. 99–114. [CrossRef]
65. Ouranidis, A.; Gkampelis, N.; Vardaka, E.; Karagianni, A.; Tsiptsios, D.; Nikolakakis, I.; Kachrimanis, K. Overcoming the solubility barrier of ibuprofen by the rational process design of a nanocrystal formulation. *Pharmaceutics* **2020**, *12*, 969. [CrossRef]
66. Karabinaki, O.; Papastylianos, S.; Padrón, N.M.; Hatzidimitriou, A.; Christofilos, D.; Arvanitidis, J. Pressure response of crystalline fluoranthene probed by Raman spectroscopy. *Crystals* **2025**, *15*, 697. [CrossRef]
67. Bridgman, P.W. Further rough compressions to 40,000 Kg/cm^2, especially certain liquids. *Proc. Am. Acad. Arts Sci.* **1949**, *77*, 129–146. [CrossRef]
68. Heimel, G.; Hummer, K.; Ambrosh-Draxl, C.; Chunwachirasiri, W.; Winokur, M.J.; Hanfland, M.; Oehzelt, M.; Aichholzer, A.; Resel, R. Phase transition and electronic properties of fluorene: A joint experimental and theoretical high-pressure study. *Phys. Rev. B* **2006**, *73*, 024109. [CrossRef]
69. Siavou, M.-T.; Siapaka, K.; Karabinaki, O.; Christofilos, D.; Arvanitidis, J. The high-pressure response of 9,9′-spirobifluorene studied by Raman spectroscopy. *Molecules* **2025**, *30*, 638. [CrossRef] [PubMed]
70. Schmidt, G.M.J. Topochemistry. Part III. The crystal chemistry of some trans-cinnamic acids. *J. Chem. Soc.* **1964**, 2014–2021. [CrossRef]
71. Wierda, D.A.; Feng, T.L.; Barron, A.R. Structure of α-*trans*-cinnamic acid. *Acta Cryst. C* **1989**, *45*, 338–339. [CrossRef]